Project Report No. 531

Heating of shallow groundwater flow by conduction from a paved surface: Requirements for coldwater stream protection

by

Craig A. Taylor and Heinz G. Stefan

Prepared for

May, 2008
Minneapolis, Minnesota

Abstract

Temperatures of shallow groundwater depend on ground surface temperatures and water recharge temperatures. Important heat transfer processes that contribute to groundwater temperatures are conduction from the soil surface into the ground(water), infiltration of warm surface water, and advection by the horizontal flow in the aquifer. Shallow groundwater temperatures respond to ground surface temperatures and infiltration regimes. Both of these are modified by urban development and climate change. In this paper we explore concepts and relationships by which shallow groundwater temperature change can be analyzed or predicted. We estimate the projected seasonal temperature change in an aquifer of given depth, thickness and flow velocity (permeability) and below a vegetated (grassy) surface when a paved surface (parking lot) of given size is added on the ground surface. The analysis is in 2-D, and groundwater temperatures are simulated as a function of horizontal and vertical distance in the aquifer, and as a function of time of the year. Results are explained and presented in a form useful for practical applications, and examples are presented.

Table of Contents

1. Introduction

Coldwater streams in a natural or agricultural landscape often provide habitat for trout. They are threatened when urban development encroaches into the watershed. The threats are related to changes in hydrology and rising water temperatures. The water source for many coldwater streams is groundwater from shallow aquifers (Figure 1.1). Shallow aquifers often depend on local infiltration and recharge. They are also heated and cooled from the ground surface.
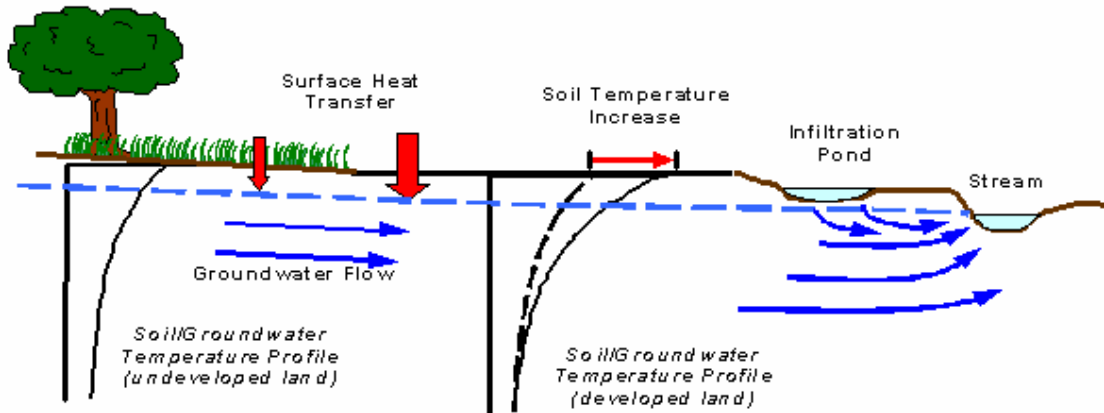

Figure 1.1 Schematic of shallow groundwater aquifer feeding a coldwater stream, before and after urban development. The groundwater is heated from the ground surface (from W. Herb).

Surface cover affects ground surface temperatures and, hence, the temperatures below the surface. Asphalt surfaces have much lower reflectivity than surfaces with plant cover, and therefore reach much higher surface temperatures during summer when solar radiation levels are high. Asphalt surfaces have both higher mean annual temperature (T_m) and higher seasonal temperature amplitude (ΔT) than surfaces with vegetation covers under the same climate conditions. Grass provides enough shade to maintain surface temperatures similar to agricultural or undeveloped land (Herb et al. 2006). As a result, most vegetated surfaces have similar surface temperature regimes regardless of the type of vegetation (Figure 1.2).
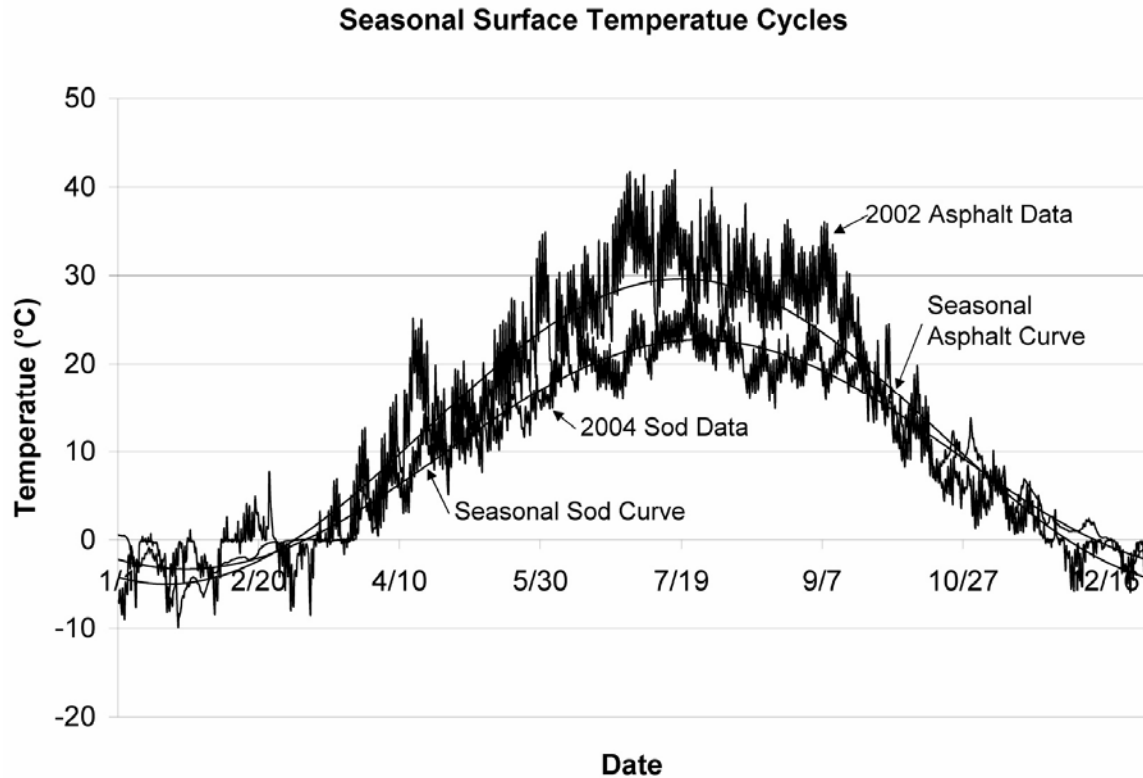
Seasonal Surface Temperatue Cycles

Figure 1.2 Seasonal cycles of asphalt and grass surface temperatures in the Twin Cities.

A network of roads, driveways and parking lots constructed in a new urban development creates areas with substantially higher mean ground surface temperatures in summer than is typical for undeveloped or agricultural (vegetated) land. These surface areas heat the soil and the shallow groundwater below by conduction. In winter, paved surfaces and vegetated surfaces are likely to have similar temperatures, especially if they are covered by snow. If they are cleared of snow paved surfaces are likely to be warmer on sunny days and cooler at night or on cloudy days.

The construction of residential or commercial buildings also has an impact on ground surface temperatures that in turn affect groundwater. In the composite landscape of an urban environment, complex interactions exist between the warmer or cooler ground surface areas and the shallow groundwater. The net effect is most likely the heating of the soil and of shallow aquifers to temperatures above predevelopment conditions (Taniguchi and Uemura 2005, Taylor and Stefan 2008).

In this study we address the question "What horizontal distance is required downstream from a paved surface such that the shallow groundwater does not feel the presence of the warmer surface?" Figure 1.1 is a basic depiction of the system. It is a vertical section through a shallow aquifer that feeds a coldwater stream. To determine this distance at which there is negligible shallow

5

groundwater temperature change, we consider the case of a single asphalt strip (e.g. a road or parking lot) bordered on each side by a large vegetated (grass) surface. Figure 1.3 illustrates this simplified condition.
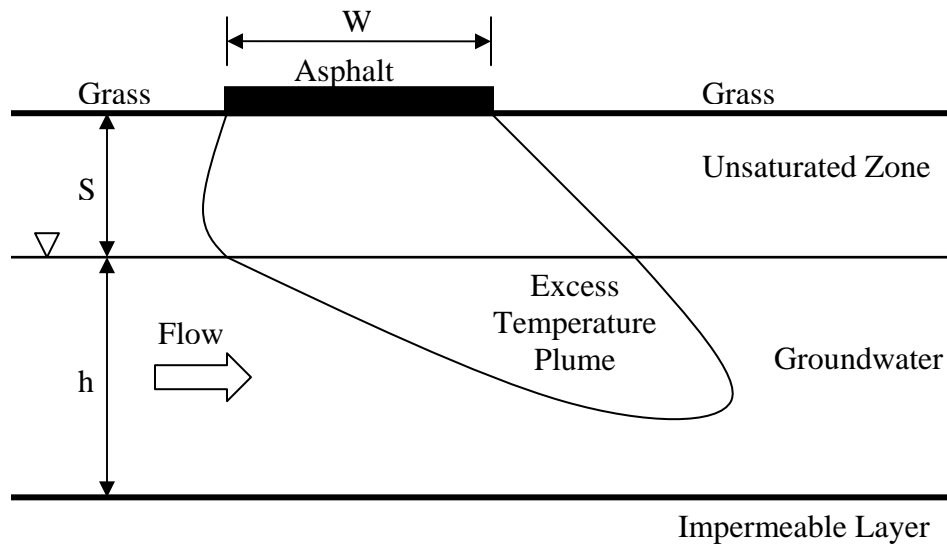

Figure 1.3 Illustration of a shallow groundwater flow being heated by an asphalt strip bordered on either side by grass.

The higher surface temperature of the asphalt strip causes a warmer temperature plume to form. The plume originates from the asphalt strip then penetrates into the groundwater where it is swept downstream under the adjacent grass surface. To quantify the heating of the groundwater due to the asphalt strip, we introduce the concept of an excess temperature. The excess temperature is the maximum temperature difference throughout the season between the local temperature with the asphalt strip and the local temperature without the asphalt strip for any given point in the domain. The excess temperature plume tracks the excess temperatures throughout the domain and can be used to determine a maximum distance at which the groundwater no longer feels the effects of the asphalt strip.

2. Formulation of model for groundwater temperature field

2.1 Basic heat transport equation

The temperature plume in the groundwater can be described by the 2D heat advection/dispersion equation (1). This governing equation includes dispersion both vertically in the soil/groundwater (z-direction) and horizontally in the direction of the groundwater flow assumed parallel to the ground surface (x-direction). We assume that the groundwater flow in the shallow aquifer is at a

uniform velocity. The groundwater table is approximated as flat and parallel to the surface.

$$\frac{\partial T}{\partial t} + u\frac{\partial T}{\partial x} = \alpha_x \frac{\partial^2 T}{\partial x^2} + \alpha_z \frac{\partial^2 T}{\partial z^2} \qquad (1)$$

where: T = temperature (°C)
   t = time (day)
   x = distance in the direction of groundwater flow (m)
   z = vertical distance from the surface (m)
   u = groundwater velocity in the x direction
   α_x = thermal diffusivity (dispersivity) in the x direction (m^2/day)
   α_z = thermal diffusivity (dispersivity) in the z direction (m^2/day)

2.2 Boundary and Initial Conditions

The local temperatures in the domain illustrated in Figure 1.3 are given by the solution $T(x,y,t)$ of equation (1) . The upper boundary condition in Figure 1.3 is the seasonal surface temperature cycle $T(x,0,t)$, which will approximated by a cosine wave. The equations for the upper boundary conditions for the grassed surface (equation 2a) and for the asphalt strip (2b) are of the same form, but the mean surface temperatures and seasonal temperatures amplitudes of grass and asphalt are different (Taylor and Stefan 2008, Herb et al. 2006). The reason is that ground surface temperatures are determined from a heat balance at that surface, and the heat flux terms for radiation, convection, conduction, and evaporation used in that heat balance are vastly different for asphalt and grass surfaces It is assumed that the ground surface temperatures T(x,0,t) in the grass and asphalt regions are spatially uniform.

The bottom boundary, at a depth $z = h$ of the aquifer, is assumed to be adiabatic ($\partial T/\partial z = 0$), i.e. vertical heat transfer has vanished. The downstream boundary condition is that the groundwater temperature is no longer changing in the x-direction ($\partial T/\partial x = 0$). The upstream boundary condition $T(0,z,t)$ is a given temperature profile $T(z,t)$ defined by the one-dimensional solution for the soil and groundwater temperatures for an infinitely long grass surface as discussed by Taylor and Stefan (2008). That temperature profile also has a seasonal periodicity.

$$\text{Grass:} \qquad T = T_{m,g} + \Delta T_g \cdot \cos\left(2\pi\frac{t}{t_0}\right) \qquad (2a)$$

$$\text{Asphalt:} \qquad T = T_{m,A} + \Delta T_A \cdot \cos\left(2\pi\frac{t}{t_0}\right) \qquad (2b)$$

where: t_0 = period (365 days)
   $T_{m,g}$ = mean annual temperature of grass surface (°C)

ΔT_g = seasonal temperature amplitude of grass surface (°C)
$T_{m,A}$ = mean annual temperature of asphalt surface (°C)
ΔT_A = seasonal temperature amplitude of asphalt surface (°C)

As initial condition it is assumed that the entire domain has a spatially uniform temperature equal to the mean annual temperature of the grass surface. Since the system is quasi-steady state the initial condition is arbitrary. The model is run through several cycles to allow time for the system to initialize before any results are recorded. The number of initializing cycles is dependent on groundwater velocity and the size of the domain (i.e. the residence time of the domain).

2.3 Normalized heat transport equation

To reduce the number of variables of the problem, a normalized (dimensionless or unitless) form of the governing heat transport equation is generated with the following dimensionless variables.

$$T^* \equiv \frac{T - T_{m,g}}{\Delta T_g}, t^* \equiv \frac{t}{t_0}, x^* \equiv \frac{x}{S}, z^* \equiv \frac{z}{S} \tag{3}$$

where: S = distance from the ground surface to the groundwater table (m). The reference length is S, the reference time t_0 is the annual period (365 days), and the reference temperature is ΔT_g is the seasonal temperature amplitude of the grass surface.

Substituting the dimensionless variables (3) into the governing equation (1) gives equation (4).

$$\frac{\Delta T_g}{t_0} \frac{\partial T^*}{\partial t^*} + \frac{1}{t_0} \frac{\partial T_{m,g}}{\partial t^*} + \frac{u \Delta T_g}{S} \frac{\partial T^*}{\partial x^*} + \frac{u}{S} \frac{\partial T_{m,g}}{\partial t^*} = \ldots$$
$$= \frac{\alpha_x \Delta T_g}{S^2} \frac{\partial^2 T^*}{\partial x^{*2}} + \frac{\alpha_x}{S^2} \frac{\partial^2 T_{m,g}}{\partial x^{*2}} + \frac{\alpha_z \Delta T_g}{S^2} \frac{\partial^2 T^*}{\partial z^{*2}} + \frac{\alpha_z}{S^2} \frac{\partial^2 T_{m,g}}{\partial z^{*2}} \tag{4}$$

Since the mean annual surface temperature (T_m) is constant, its derivative terms are equal to zero. The dimensionless governing equation can then be simplified to equation (5).

$$\frac{\partial T^*}{\partial t^*} + u^* \frac{\partial T^*}{\partial x^*} = \alpha_x^* \frac{\partial^2 T^*}{\partial x^{*2}} + \alpha_z^* \frac{\partial^2 T^*}{\partial z^{*2}} \tag{5}$$

where: $u^* \equiv \frac{u \cdot t_0}{S}$ = normalized groundwater velocity

8

$$\alpha_x^* \equiv \frac{\alpha_x \cdot t_0}{S^2} = \text{normalized thermal diffusivity in the } x\text{-direction}$$

$$\alpha_z^* \equiv \frac{\alpha_z \cdot t_0}{S^2} = \text{normalized thermal diffusivity in the } z\text{-direction}$$

It is important to note that equation (5) written for the dimensionless variables defined by equation(s) (3) has three dimensionless parameters (u^*, α^*_x and α^*_z) which, when changed, will give different numerical solutions for the dimensionless groundwater temperature T^*.

It is also important to note that the diffusivities in the groundwater and in the dry soil above the groundwater table are different. Equation (5) will apply to both of these regions. The different diffusivities are distinguished by adding a subscript 'D' for dry soil and 'G' for groundwater. Because there is no groundwater in the region of the dry soil, the velocity term in the dry soil will be set equal to zero ($u^* = 0$).

2.4 Normalized Boundary Conditions

Using the dimensionless variables (3) in the equation (2) gives equation (6) which is the dimensionless form of the upper boundary condition for the grass regions. The upper boundary condition for the asphalt strip can be made dimensionless by the same method, but mean surface temperature and seasonal amplitude need to be adjusted to place them in the same scale as the dimensionless variables. Equation (7) is the dimensionless form of the upper boundary condition for the asphalt strip.

$$T^* = \cos\left(2\pi \cdot t^*\right) \tag{6}$$

$$T^* = \left(\frac{T_{m,A} - T_{m,g}}{\Delta T_g}\right) + \frac{\Delta T_A}{\Delta T_g} \cdot \cos\left(2\pi \cdot t^*\right) \tag{7}$$

To fit the dimensionless variables (3) the domain also has to be modified. The width of the asphalt strip W and the thickness of the aquifer h are not direct boundary conditions for equation (5), but they have to be normalized to $W^* = W/S$ and $h^* = h/S$ to define the normalized domain for which the normalized temperature field will be calculated.

2.5 Discretization and solution of the normalized heat transport equation

The dimensionless governing equation (5) can be solved numerically using an alternating direction implicit method with a central difference scheme spatially, and a forward difference scheme temporally. This method solves for temperatures throughout the domain using two halftime steps. The first half time

step solves (updates) in the x-direction, while the second halftime step solves in the y-direction. The dimensionless governing equation (5) is discretized and the solution method is discussed in Appendix A. Because the initial conditions are arbitrary, the solution is run for several years until a quasi-steady state condition is achieved. The discretized spatial steps in the horizontal (flow direction) and vertical directions are 0.1, The computational time step, ranging between 0.001 and 0.000001, is adjusted on a case by case basis to minimize both error and computational run time.

3. Example Solutions

Although the problem is solved using dimensionless variables examples will be presented in their dimensional form for illustration. First consider a 200m wide asphalt strip in an otherwise vegetated (grass-covered) surface. The aquifer below this surface is 20m thick and the groundwater table is one meter below the ground surface. The groundwater flows at a velocity u = 2m/day. The thermal diffusivities are estimated as follows: in the unsaturated soil above the water table ($\alpha_{Dx} = \alpha_{Dy} = 0.07m^2/day$) and in the groundwater ($\alpha_{Gx} = 0.42m^2/day$, $\alpha_{Gy} = 0.14m^2/day$).

The diffusivity in the unsaturated zone is assumed to be similar to the diffusivity found in the soil at the University of Minnesota, St. Paul campus weather station (Baker and Baker 2002, Taylor and Stefan 2008). The diffusivity in the groundwater in the x-direction is magnified by a multiple of six due to saturated pore spaces and longitudinal hydrodynamic dispersion (See Bear 1972 or appendix of Taylor and Stefan 2008). The diffusivity in the groundwater in the z-direction is one-third of the diffusivity in the x-direction because of the ratio of transverse to longitudinal hydrodynamic dispersion. Hydrodynamic dispersion in the groundwater is best described by a dispersion tensor; however a ratio of 1:3 (transverse: longitudinal) has been used as a reasonable approximation (Zheng and Bennett 1995, Benekos 2005, Qian and Stefan 2008, and Taylor and Stefan 2008).

The upper boundary condition for the asphalt strip (7) depends on the differences in the seasonal surface temperature parameters between an asphalt surface and a grass surface. Since the boundary condition is for a seasonal cycle the period (t_0) is set to 365 days. Values chosen for the temperature parameters were typical of central Minnesota ($T_{m,A}$ = 12.3°C, $T_{m,g}$ = 9.7°C, ΔT_A = 17.3°C, ΔT_g = 13.0°C). This results in the following upper boundary condition for the asphalt strip:

$$T^* = 0.2 + 1.33 \cdot \cos\left(2\pi \cdot t^*\right) \tag{8}$$

Using the 1-D solution for temperatures below a grass surface (Taylor and Stefan 2008), the temperature penetration profiles and the maximum seasonal temperatures under the grass surface were determined (Figures 3.1 and Figure 3.2, respectively).
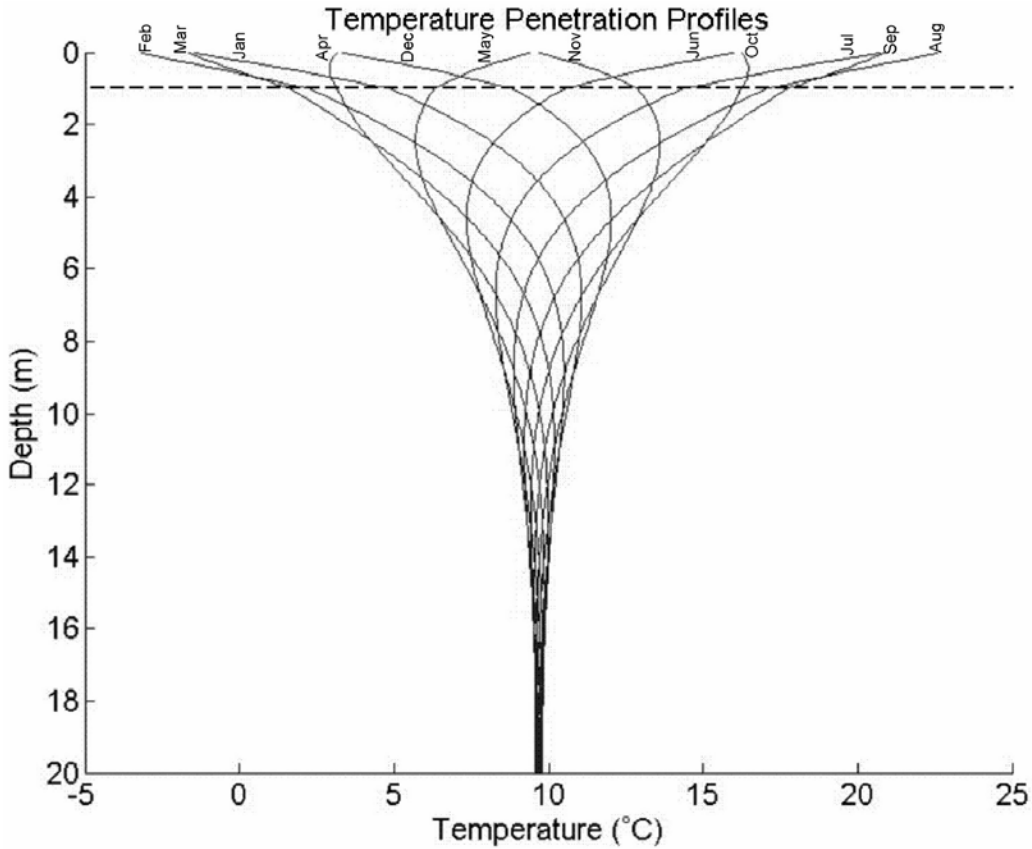
Figure 3.1 Temperature penetration profiles under a grass surface (S = 1.0m, h = 20m, $\alpha_{Dx} = \alpha_{Dy} = 0.07m^2/day$, $\alpha_{Gx} = 0.42m^2/day$, $\alpha_{Gy} = 0.14m^2/day$, $T_{m,g} = 9.7°C$, and $\Delta T_g = 13.0°C$)
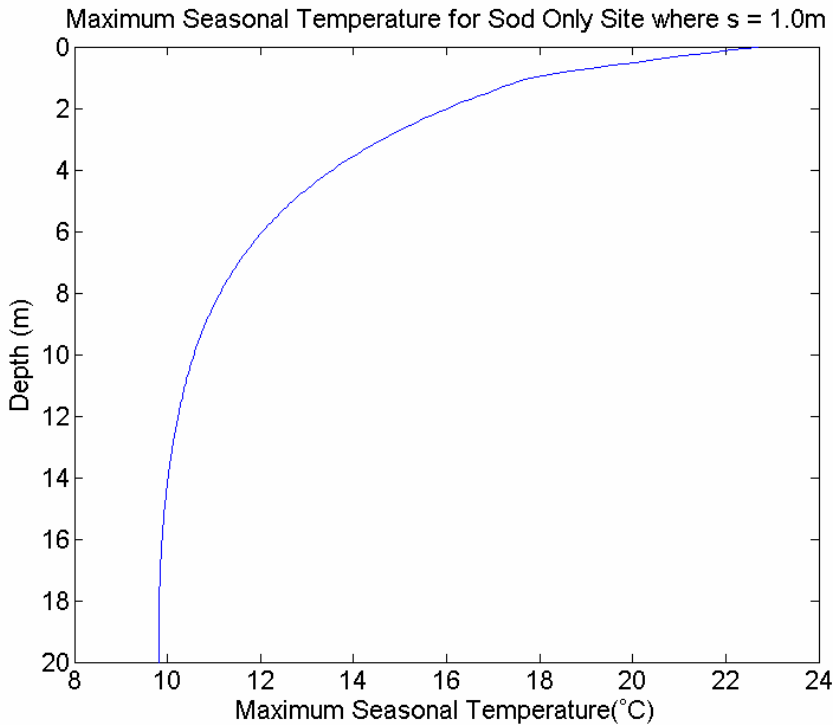
Figure 3.2 Maximum annual temperatures ($°C$) under a grass surface ($S = 1.0m$, $h = 20m$, $\alpha_{Dx} = \alpha_{Dy} = 0.07m^2/day$, $\alpha_{Gx} = 0.42m^2/day$, $\alpha_{Gy} = 0.14m^2/day$, $T_{m,g} = 9.7°C$, and $\Delta T_g = 13.0°C$).

The 2D solution scheme discussed in Section 2.5 was used to calculate the local soil or groundwater temperatures in the domain throughout the entire annual cycle. Four snapshots of the temperature field at 3-month intervals are given in Figures 3.3 a-d. The left-hand edge of each plot at x = -300m in Figures 3.3 a-d shows the temperature distribution below an infinite grass surface. By comparing the entire plot to the 1D grass only solution on the left edge of the plot, the extent of the temperature penetration from the asphalt can be gauged.

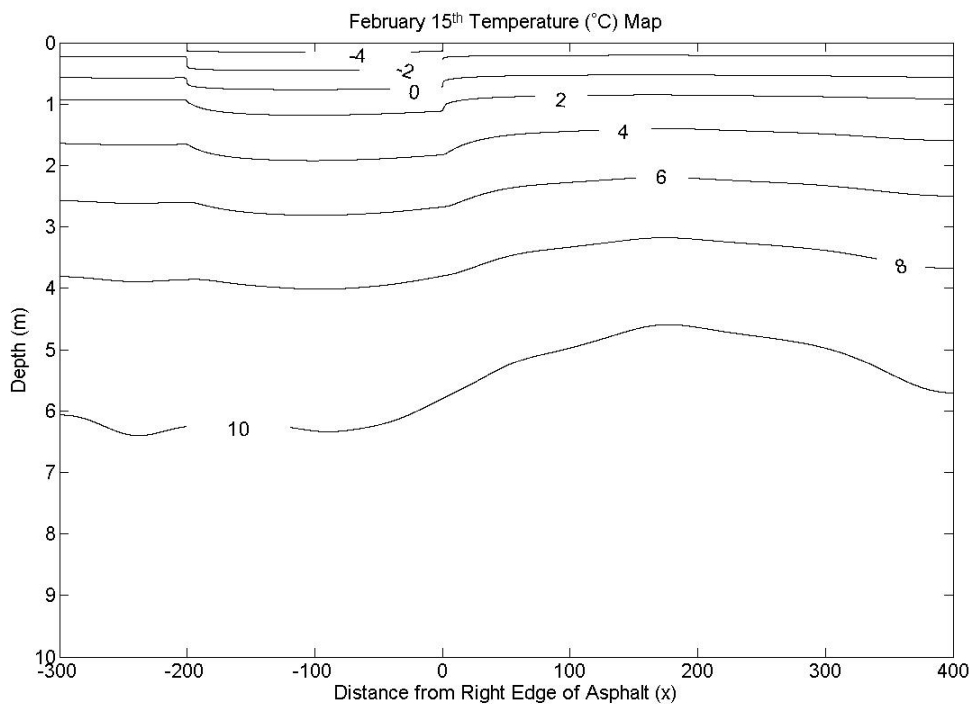February 15th Temperature (°C) Map

Figure 3.3a Instantaneous temperature field given by isotherms in the unsaturated zone and groundwater domain for February 15. Asphalt extends from $x = -200m$ to $0m$. Groundwater is flowing in the x-direction. Parameter values are: $W = 200m$, $S = 1.0m$, $h = 20m$, $u = 1.0m/day$, $\alpha_{Dx} = \alpha_{Dy} = 0.07m^2/day$, $\alpha_{Gx} = 0.42m^2/day$, and $\alpha_{Gy} = 0.14m^2/day$.
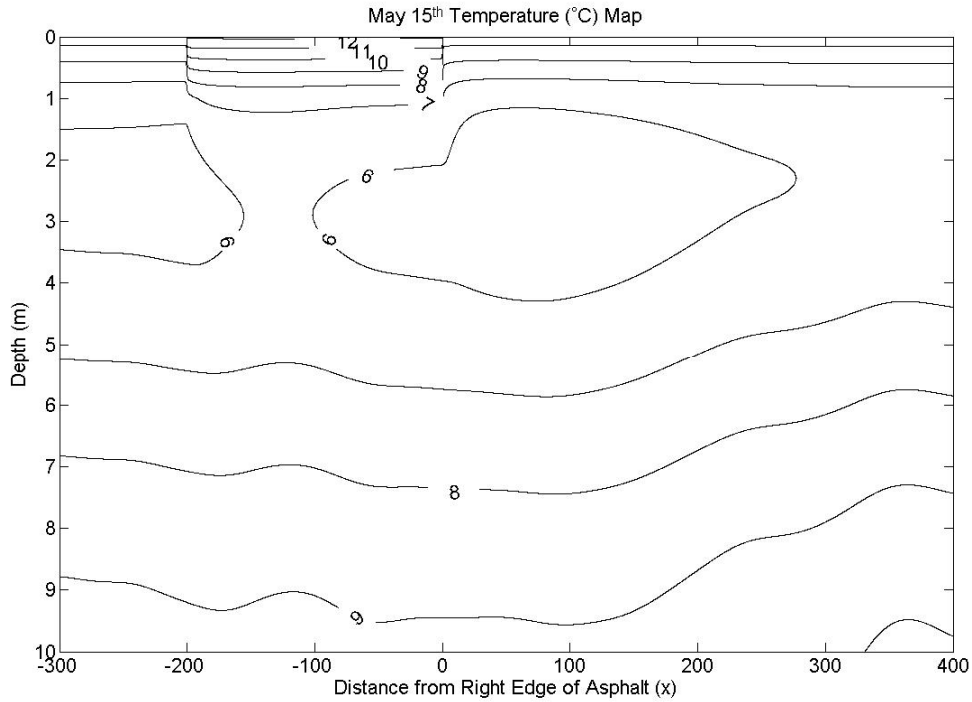
May 15th Temperature (°C) Map

Figure 3.3b Instantaneous temperature field given by isotherms in the unsaturated zone and groundwater domain for <u>May 15</u>. Asphalt extends from $x = -200m$ to $0m$. Groundwater is flowing in the x-direction. Parameter values are: $W = 200m$, $S = 1.0m$, $h = 20m$, $u = 1.0m/day$, $\alpha_{Dx} = \alpha_{Dy} = 0.07m^2/day$, $\alpha_{Gx} = 0.42m^2/day$, and $\alpha_{Gy} = 0.14m^2/day$.

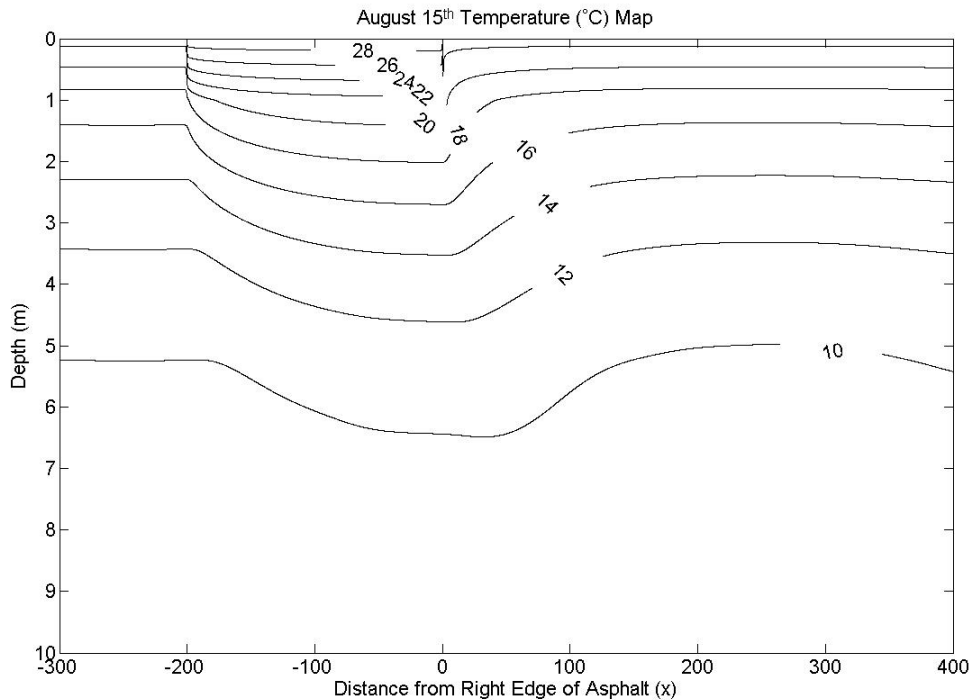August 15th Temperature (°C) Map

13

Figure 3.3c Instantaneous temperature field given by isotherms in the unsaturated zone and groundwater domain for <u>August 15</u>. Asphalt extends from $x = -200m$ to $0m$. Groundwater is flowing in the x-direction. Parameter values are: $W = 200m, S = 1.0m, h = 20m, u = 1.0m/day, \alpha_{Dx} = \alpha_{Dy} = 0.07m^2/day, \alpha_{Gx} = 0.42m^2/day,$ and $\alpha_{Gy} = 0.14m^2/day$.
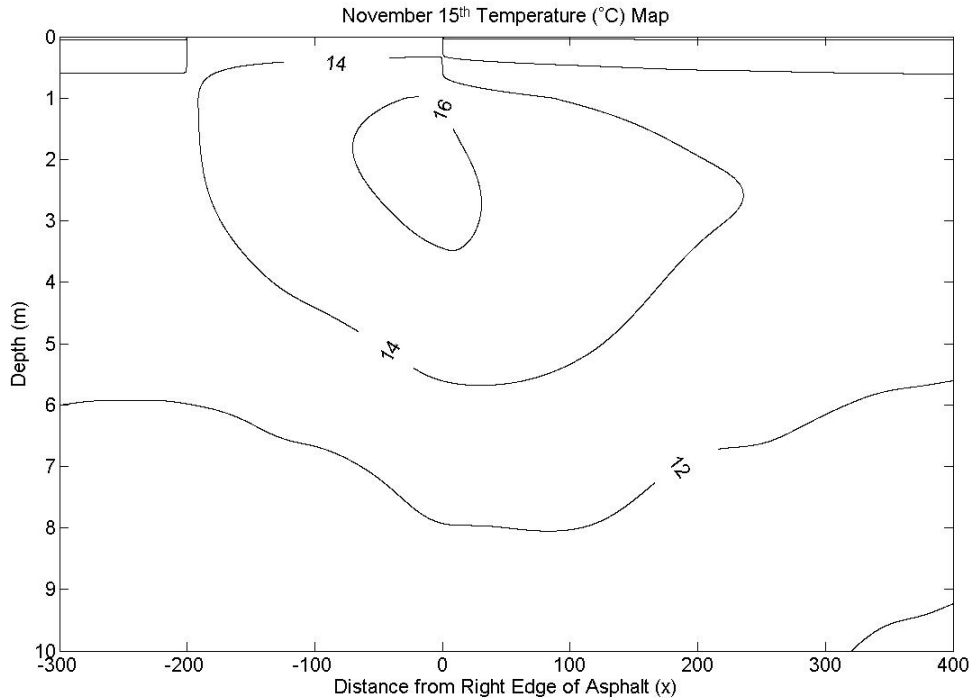

November 15th Temperature (°C) Map

Figure 3.3d Instantaneous temperature field given by isotherms in the unsaturated zone and groundwater domain for <u>November 15</u>. Asphalt extends from $x = -200m$ to $0m$. Groundwater is flowing in the x-direction. Parameter values are: $W = 200m, S = 1.0m, h = 20m, u = 1.0m/day, \alpha_{Dx} = \alpha_{Dy} = 0.07m^2/day, \alpha_{Gx} = 0.42m^2/day,$ and $\alpha_{Gy} = 0.14m^2/day$.

The 2D solution scheme discussed in Section 2.5 was also used to determine the maximum annual temperatures at each point of the entire domain. Figure 3.4 is an example of these maximum temperatures and illustrates how the warmer asphalt surface temperatures propagate downwards through the soil into the aquifer, and how the warmer water is carried away by the flow. The left-hand edge of Figure 3.4 at x = -300m shows the temperature distribution below a grass surface previously given in Figure 3.1. The mechanisms of heat transport in the system are reflected in the shapes of the isotherms. The "dips" in the isotherms are due to heat diffusing vertically downward from the asphalt surface. The horizontal widening of the "dips" with depth into the aquifer is due to the effective diffusion of the penetrating heat. Below the groundwater table, i.e. $z > 1m$, the "dips" translate to the right with depth due to advection in the groundwater. The bends in the 20 and 22-degree isotherms as they cross the groundwater table reflect the difference in the effective diffusivity between the saturated and unsaturated zones.
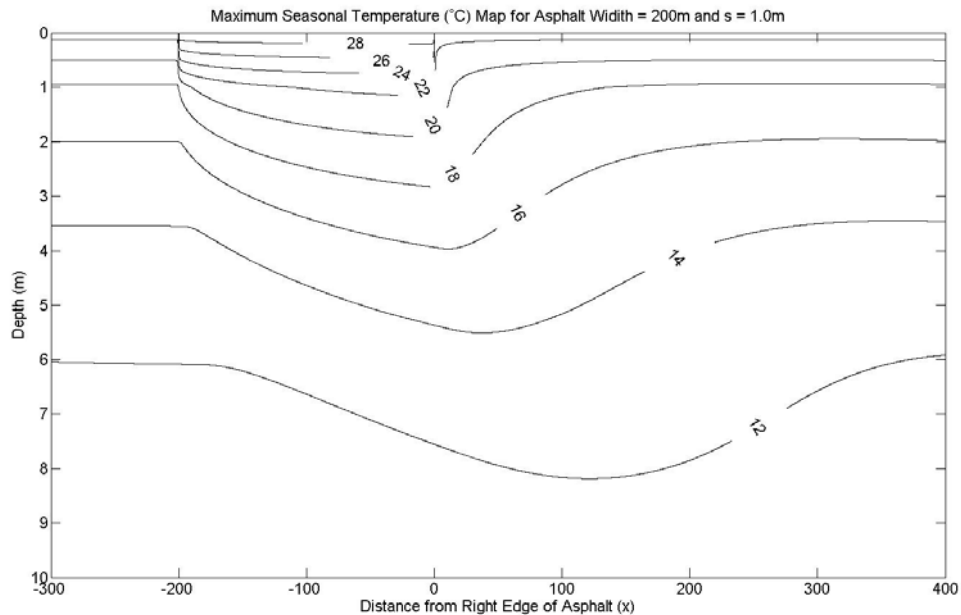
14

Figure 3.4 Maximum seasonal temperatures ($°C$) below composite grass-asphalt-grass surface. The groundwater is flowing in the positive x-direction. The downstream (right) edge of the asphalt strip is located at $x = 0$. Parameter values are: $W = 200m$, $S = 1.0m$, $h = 20m$, $u = 2.0m/day$, $\alpha_{Dx} = \alpha_{Dy} = 0.07m^2/day$, $\alpha_{Gx} = 0.42m^2/day$, and $\alpha_{Gy} = 0.14m^2/day$.

In the next computational step, the temperature at each point in the domain computed for each time step in the annual cycle was compared to the 1D grass only solution at the same depth and time, and the temperature difference between the composite site (grass-asphalt-grass) and the grass only site was then calculated for each point in the domain and each time step. The maximum of these instantaneous temperature differences was then recorded for each point and plotted in Figure 3.5. The region where there are higher temperatures for the composite site than for the grass only site can be thought of as an "excess temperature plume." A review of the results in Figure 3.5 indicates that at distance greater than 300m downstream of the asphalt, the maximum annual temperature at any depth is less than 0.5°C higher than the maximum annual temperature for a grass only site at that same depth. The penetration depth of the 0.5°C maximum annual excess temperature is about 12m.
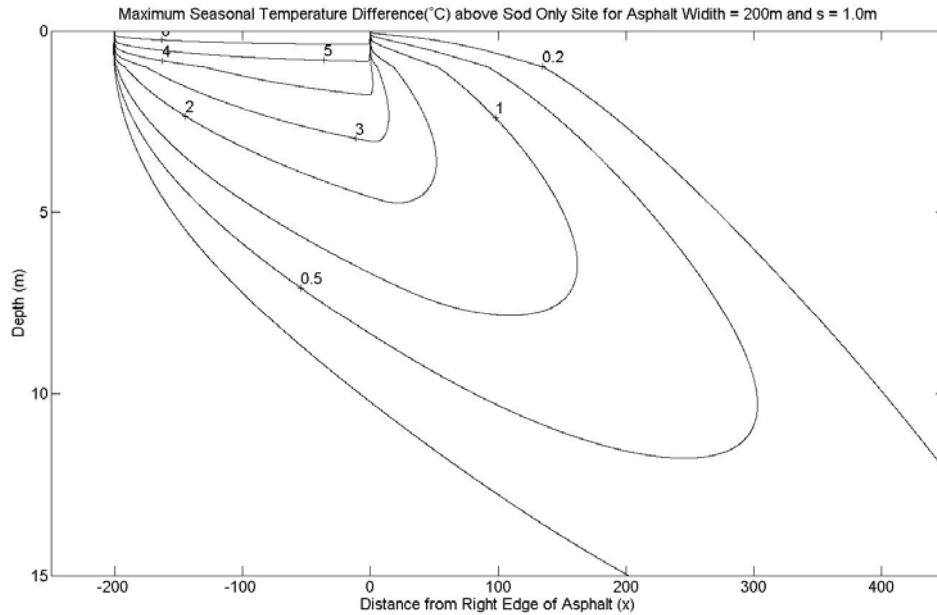
15

Figure 3.5 Excess temperature plume for a composite grass-asphalt-grass surface cite. The excess temperature ($°C$) is the increment above the temperature of a grass only site at the same location/depth. ($W = 200m$, $s = 1.0m$, $h = 20m$, $u = 2.0m/day$, $\alpha_{Dx} = \alpha_{Dy} = 0.07m^2/day$, $\alpha_{Gx} = 0.42m^2/day$, and $\alpha_{Gy} = 0.14m^2/day$)

In order to evaluate the effect of the size of a paved surface (parking lot) and of the groundwater velocity on the temperature field, the model was run again with the same parameter values, except that the asphalt width and velocity were reduced by half, i.e. $W = 100m$ and $u = 1.0m/day$. The maximum annual temperatures for the grass only site are the same as in Figure 3.2). The maximum annual temperatures for the composite (grass-asphalt-grass) site and the excess temperature plume do change, however. They are shown in Figure 3.6 and Figure 3.7, respectively.
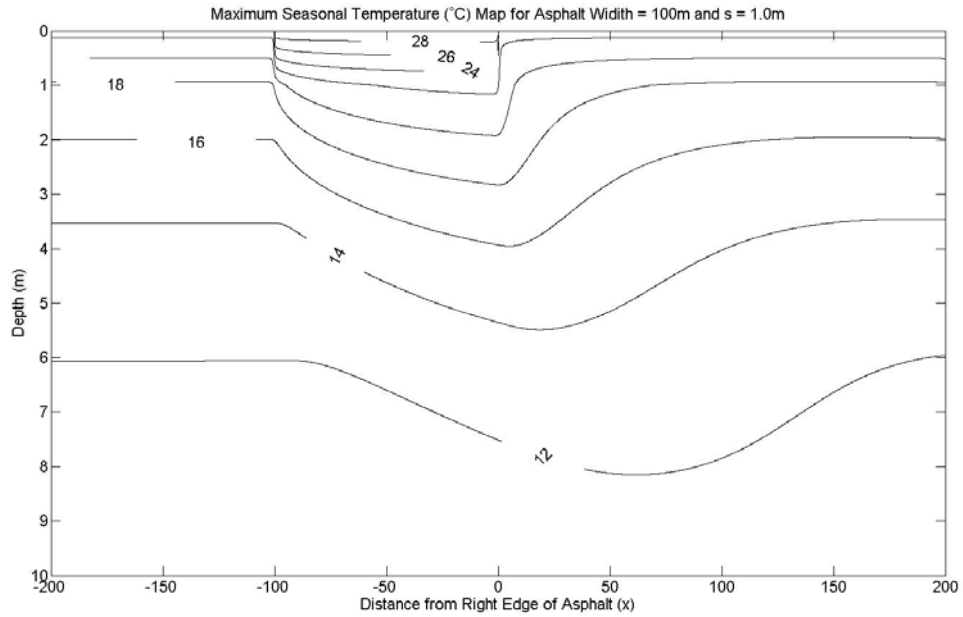
16

Figure 3.6 Maximum annual temperatures (°C) below a grass-asphalt-grass surface. Asphalt extends from *-100m* to *0m* in *x*-direction. The downstream (right) edge of the asphalt strip is located at $x = 0$. Groundwater is flowing in the *x*-direction. Parameter values are: $W = 100m$, $S = 1.0m$, $h = 20m$, $u = 1.0m/day$, $\alpha_{Dx} = \alpha_{Dy} = 0.07m^2/day$, $\alpha_{Gx} = 0.42m^2/day$, and $\alpha_{Gy} = 0.14m^2/day$.
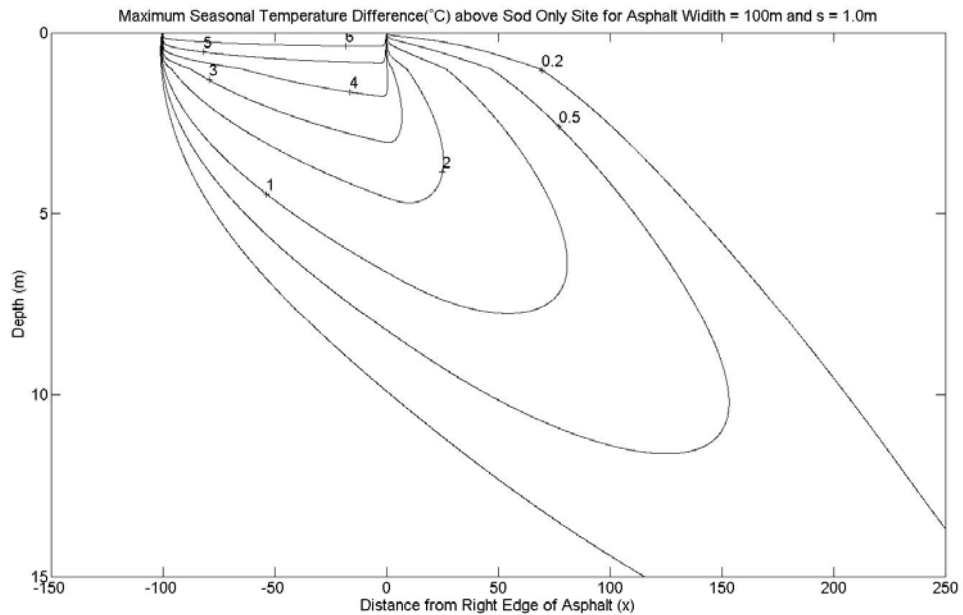

Figure 3.7 Excess temperature plume for a composite grass-asphalt-grass surface cite. The excess temperature (°C) is the degrees above the temperature of a grass only site at the same location/depth. Parameter values are: $W = 100m$,

17

$s = 1.0m$, $h = 20m$, $u = 1.0m/day$, $\alpha_{Dx} = \alpha_{Dy} = 0.07m^2/day$, $\alpha_{Gx} = 0.42m^2/day$, and $\alpha_{Gy} = 0.14m^2/day$.

A comparison of Figure 3.4 with Figure 3.6 and of Figure 3.5 with Figure 3.7 indicates that the wider asphalt strip and the higher groundwater velocity have little effect on the excess temperature penetration depths. The penetration depth of the $0.5°C$ contour is still about 12m after the asphalt strip width has been cut in half. The narrower asphalt strip and lower groundwater velocity significantly decrease the distance to which the excess temperature is transported downstream. Figure 3.7 indicates that the $0.5°C$ maximum annual excess temperature reaches a distance of 150m downstream of the asphalt strip. This distance was reduced by half when the asphalt width and groundwater flow velocity were reduced by half.

4. Range of values for variables and parameters

Before we develop a general and widely applicable set of solutions from the normalized equations, we need to consider a range of values for the parameters and variables in the general problem. The purpose of this section is to give these values.

There are two sets of parameters needed to solve for the groundwater temperature field: the surface temperature (annual mean, seasonal amplitude, and period) and physical properties (asphalt or parking lot width, water table depth, aquifer depth, groundwater velocity, thermal diffusivities).

Ranges of values considered for the dimensional and non-dimensional parameters are given in Tables 4.1 and 4.2, respectively. Values selected for our study are also given in Tables 4.1 and 4.2.

Table 4.1 Meaningful ranges and selected ranges of necessary variables and parameters

Variable or parameter	Range	Selected range
W (m)	1 – 1000	10 – 200
h (m)	10 – 30	20*S
S (m)	0 – 15	1 – 10
ΔT_A (°C)	14 – 20	17.3
ΔT_g (°C)	10 – 16	13.0
$T_{m,A}$ (°C)	9 – 15	12.3
$T_{m,g}$ (°C)	7 – 13	9.7
t_0 (days)	1 or 365	365
u (m/day)	0 – 200	0 – 2
α_{Dx}, α_{Dz} (m^2/day)	0.01 – 0.60	0.03 – 0.40
α_{Dx}/α_{GX}	1/10 – 1	1/10 – 1
α_{Gx}/α_{Gz}	1/10 – 1/2	1/3

Table 4.2 Possible ranges and selected ranges of necessary dimensionless variables and parameters

Variable or parameter	Range	Selected range
W^*	$1 - 1000$	$10 - 200$
h	$10 - 30$	$20*S$
$\Delta T_A / \Delta T_g$	$0.87 - 2.00$	1.33
$(T_{m,A} - T_{m,g}) / \Delta T_g$	$0 - 1.14$	0.20
u^*	$0 - 73,000$	$0 - 730$
$\alpha_{Dx}^*, \alpha_{Dz}^*$	$0.016 - 219$	$0.44 - 146$
α_{Dx}/α_{Gx}	$1/10 - 1$	$1/10 - 1$
α_{Gx}/α_{Gz}	$1/10 - 1/2$	$1/3$

A lot of consideration was given to the selected ranges of the parameters. The width of the asphalt strip (W) is limited to the reasonable width of a paved road or parking lot. The depth to the groundwater table (S) is limited by the temperature fluctuations. For depth less than $S = 1m$, the diurnal fluctuations become significant. At depths greater than $S = 10m$, the seasonal amplitude fluctuations become quite small. The seasonal mean temperatures and amplitudes for the grass and asphalt surfaces were chosen as typical values for the Twin Cities area. The period (t_0) is set as 365 days, since the seasonal cycle in the primary concern. The groundwater velocity (u) is limited by expected groundwater velocities in the region of the Vermillion River, MN, and the computational runtime of the model. The diffusivities chosen for the unsaturated zone (α_{Dx}, α_{Dz}) are similar to the diffusivity found in the soil at the University of Minnesota, St. Paul campus weather station. The ratio of vertical diffusivities between the unsaturated zone and the groundwater (α_{Dx}/α_{Gx}) is limited by the presence of water in the pore spaces, the size of the sand particles, and the groundwater velocity. The ratio of horizontal to vertical diffusivity in the groundwater (α_{Gx}/α_{Gz}) is the accepted value by Zheng and Bennett (1995), Benekos (2005), Qian and Stefan (2008)

5. Numerical results for the selected range of parameter and variable values

Default values were also chosen for the dimensionless parameters in Table 4.2. Holding all of the parameters constant at the default value, except one, it is possible to evaluate the effect of that single variable parameter on the results. The default parameters are as follows: $W^* = 100, u^* = 365, \alpha^* = \alpha_{Dx}^* = \alpha_{Dz}^* = 25.55, \alpha_{Dx}/\alpha_{GX} = 1/6$.

5.1 Excess Temperature Plots

Figures 5.1 to 5.5 give maximum annual excess temperature results in the same format. To recall, excess temperature is the temperature difference

between a local annual maximum temperature for the composite (grass-asphalt-grass) surface and the grass only surface. Each line in each figure represents the numerical simulation results for an excess temperature plume plot similar to Figures 3.5 and 3.7, except that results in Figures 5.1 to 5.4 are given in dimensionless form. In Figures 5.1 and 5.2 excess temperatures are normalized to the seasonal temperature amplitude ΔT_g according to the definition of dimensionless temperatures in equation (3). For a seasonal temperature amplitude at the grass surface of ΔT_g = 13°C, a dimensionless excess temperature of 0.05 therefore represents 0.05 x 13 = 0.65°C. Each point on the line represents the maximum excess temperature over the entire annual cycle and the entire depth of the aquifer at that the specified distance x^* downstream of the asphalt strip. Figures 5.1 to 5.4 therefore represent the worst-case excess temperature for the specified set of model input parameters.

In all four figures the excess temperatures drop off quite quickly with distance from the asphalt strip. Most noticeable in Figure 5.1, the excess temperature plot levels off for a bit before continuing to decrease. This apparent irregularity is actually caused by the lower adiabatic boundary. When the higher heat from the asphalt strip penetrates vertically through the entire domain, it is reflected by the lower adiabatic boundary back into the domain and, therefore, heats the system. This is a rather extreme case, since in a natural system the lower boundary would be bedrock or a low permeability layer (leaky layer). Both bedrock and leaky layers will have lower diffusivities than the aquifer and will reflect some, but not all, of the heat back into the system. Consequently, in a natural system, some of the heat will continue to penetrate into the system below the aquifer, thereby reducing the amount of "leveling off" observed.
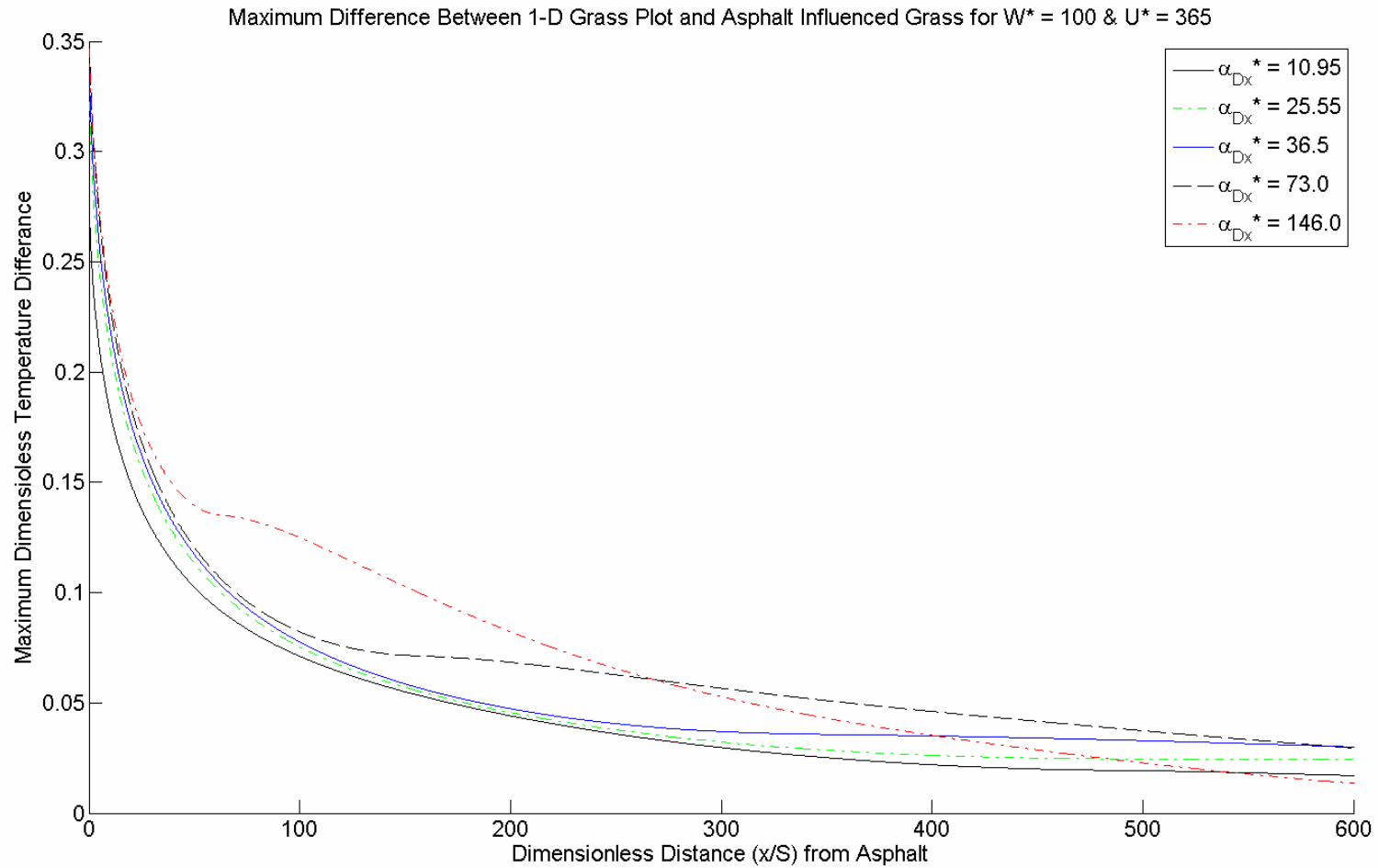
Figure 5.1 Maximum excess temperatures at any depth for the case with varying values of α_{Dx}*. All other model input parameters are specified by the default values in Table 4.2.
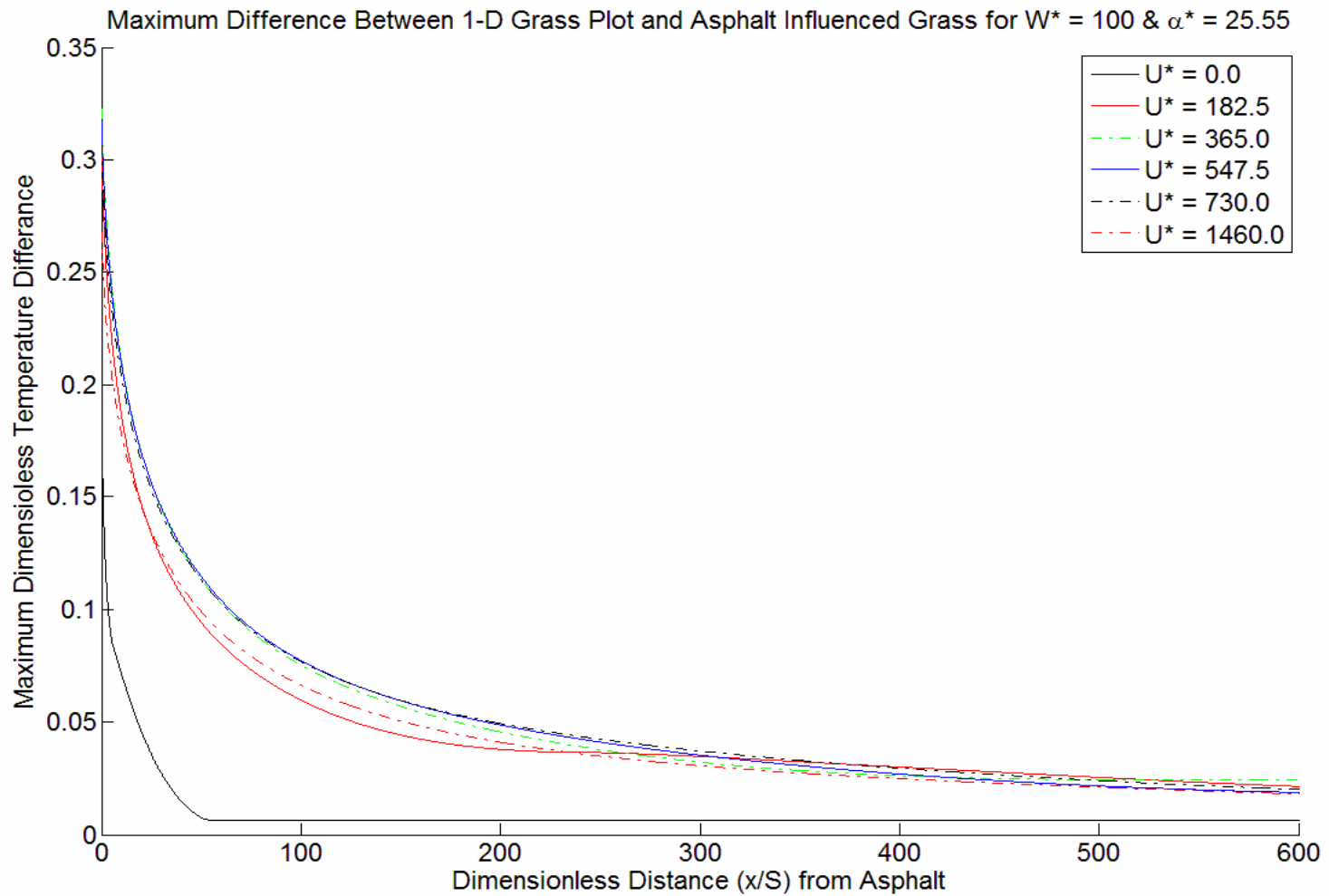
Figure 5.2 Maximum excess temperatures at any depth for the case with varying values of $U*$. All other model input parameters are specified by the default values in Table 4.2.
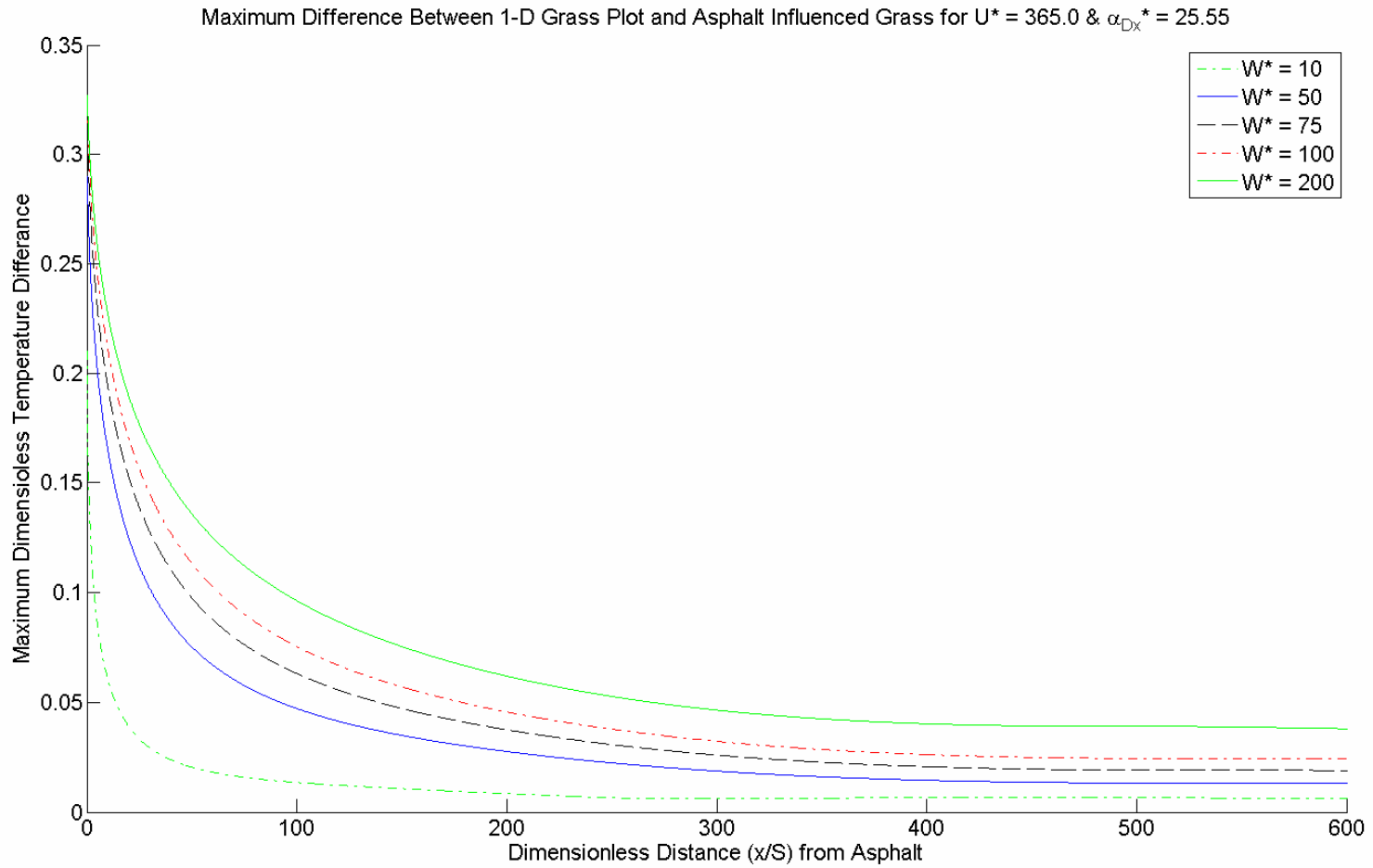
Figure 5.3 Maximum excess temperatures at any depth for the case with varying values of $W*$. All other model input parameters are specified by the default values in Table 4.2.
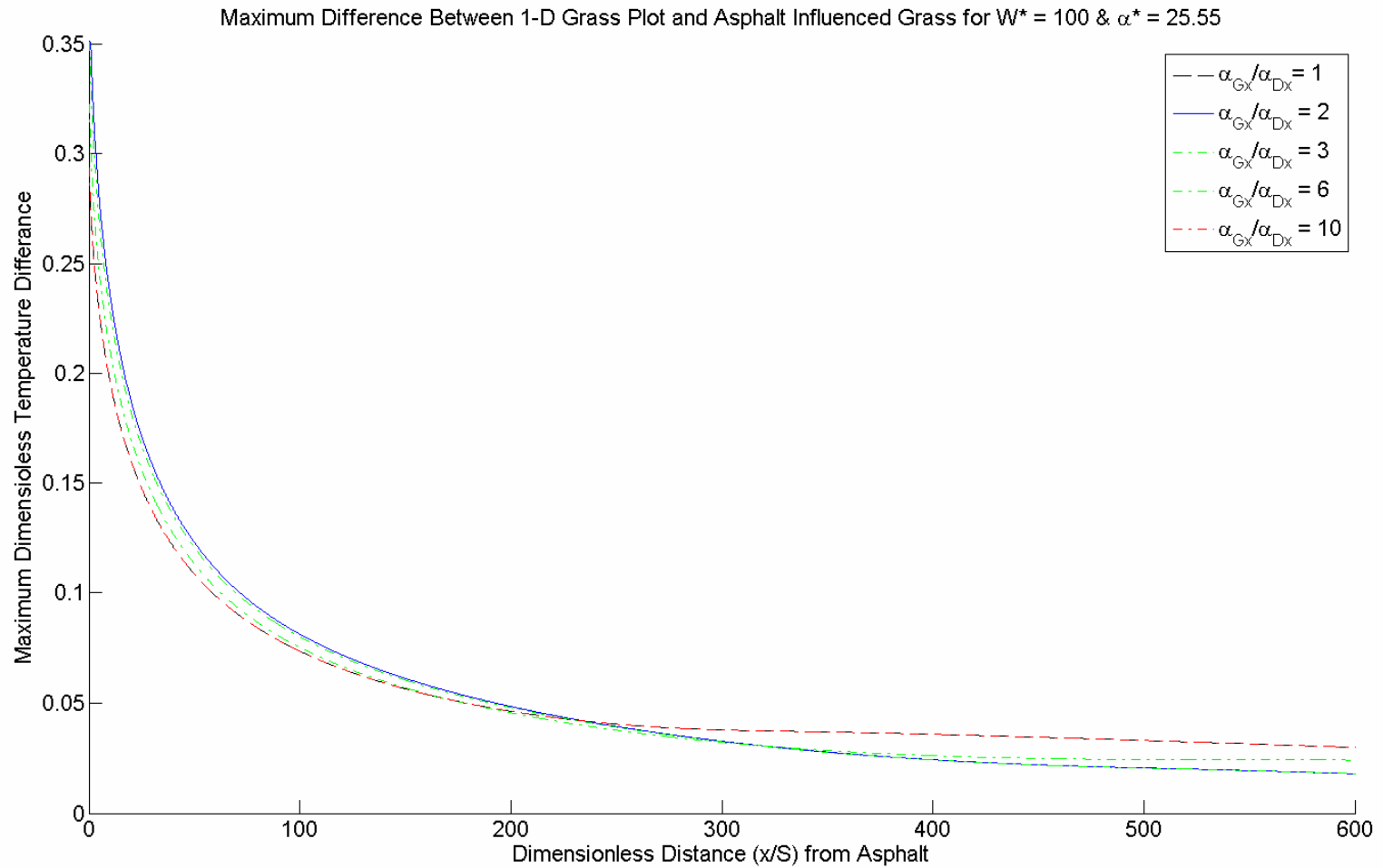
Figure 5.4 Maximum excess temperatures at any depth for the case with varying values of α_{Dx}/α_{Gx}. All other model input parameters are specified by the default values in Table 4.2.
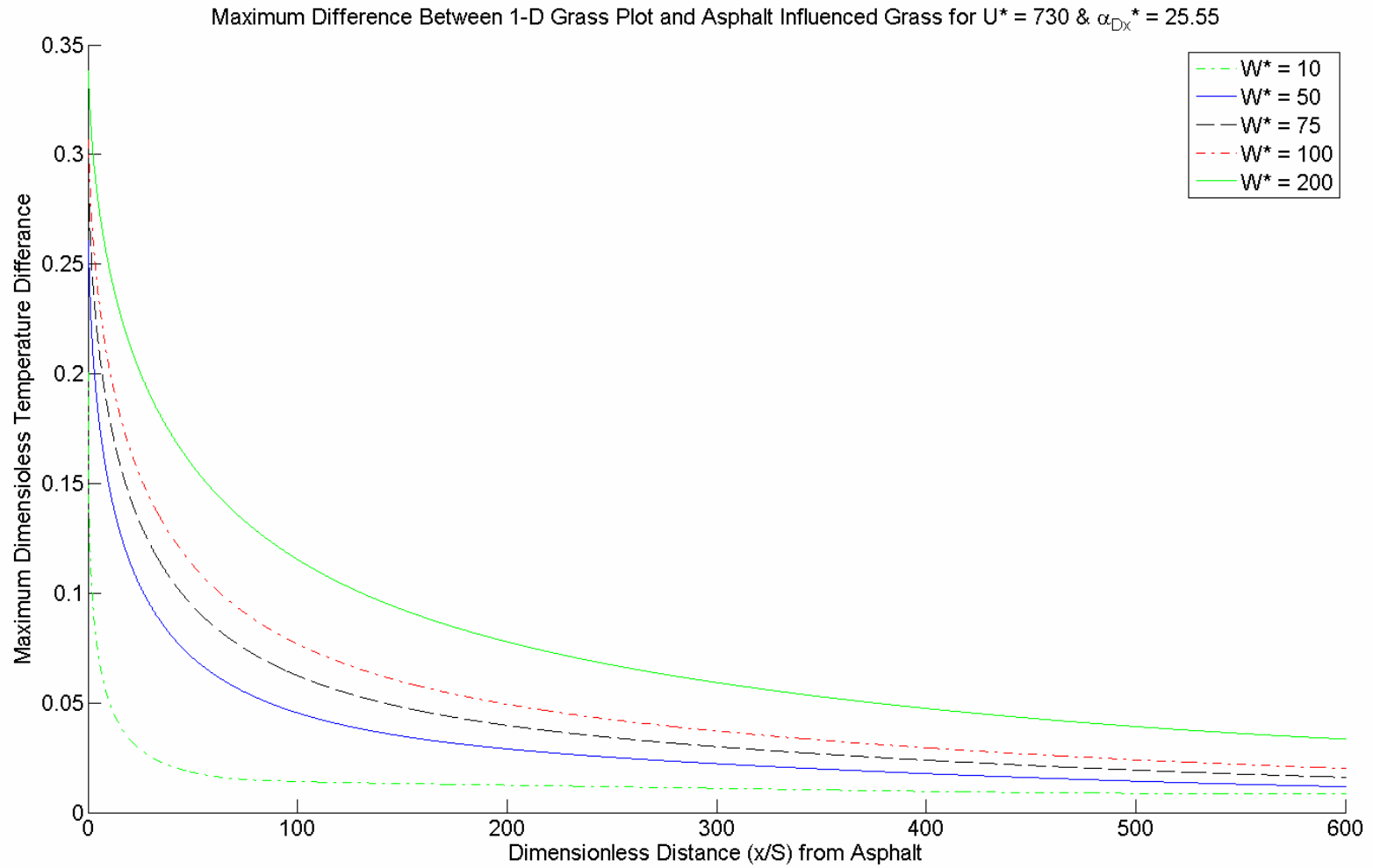
Figure 5.5 Maximum excess temperatures at any depth for the case with u* = 730 and varying values of $W*$. All other model input parameters are specified by the default values in Table 4.2.

5.2 Critical distance from asphalt surface for negligible impact

Given enough distance from the asphalt strip (paved surface) the maximum seasonal excess temperature will go to zero, meaning that the groundwater temperatures are essentially unaffected by the asphalt strip. Considering Figures 5.1 through 5.5 the distance of "zero impact" may be very substantial. Instead, it seems appropriate to consider a distance at which the presence of the asphalt strip has "little impact" on the groundwater temperatures. This critical distance is taken to be the distance at which the maximum normalized excess temperature at all depths (as defined earlier) becomes less than 0.05. In the example problem a normalized excess temperature of 0.05 equated to a dimensional excess temperature of 0.65°C. Some would, however, consider this a significant excess. It should also be noted, thought, that the groundwater only approaches the maximum excess temperature at one depth for a few days out of the year.

The critical distances, thus defined, are obtained in our simulations and are shown in Figures 5.6 to 5.9. The sudden shifts in critical distances shown in Figures 5.6 and 5.9 reflect the leveling off seen in Figures 5.1 and 5.4. These shifts are caused by reflection of heat at the lower boundary of the aquifer as explained earlier. Figure 5.7 indicates that, over the range of groundwater velocities considered, the critical distance plateaus and even decreases at higher velocities. The groundwater flow acts to push the excess temperature plume downstream. Intuitively one might expect that the critical distance would increase with higher groundwater velocities; however, a higher groundwater flow velocity also causes a smaller heat flux into the groundwater as it passes underneath the asphalt layer. Figure 5.8 indicates that the critical distance has a nearly linear dependence on the asphalt width. Figure 5.9 indicates that there is little dependence on the x-direction diffusivity ratio between the dry and saturated soil. Figures 5.6 and 5.9 suggest that the delivery rate of the surface heat to the groundwater table is more important to the critical distance than then horizontal diffusivity in the aquifer. The plateau in Figure 5.7 and the lack of dependence in Figure 5.9 speak to the complex interaction of advection and diffusion/dispersion on the transport of heat in the aquifer.
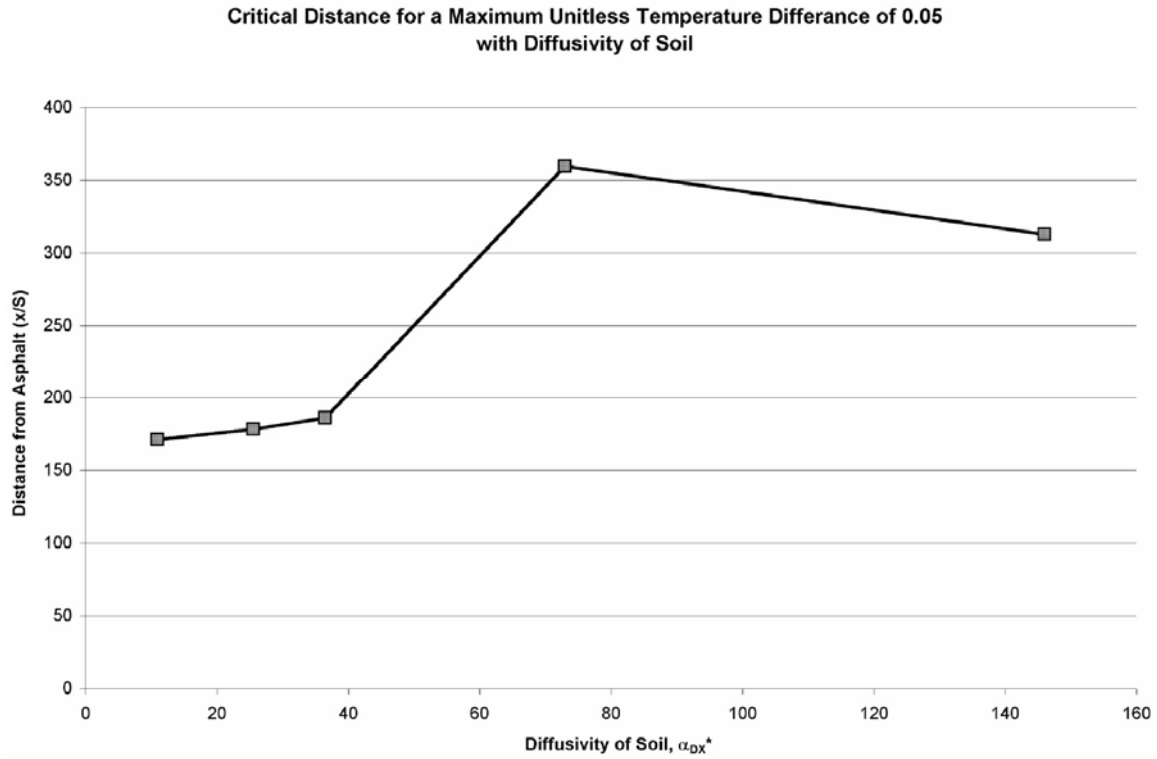
Figure 5.6 Critical normalized distance from pavement (x*) vs. normalized thermal diffusivity in the dry soil ($\alpha_{Dz}*$) (corresponding to Figure 5.1)

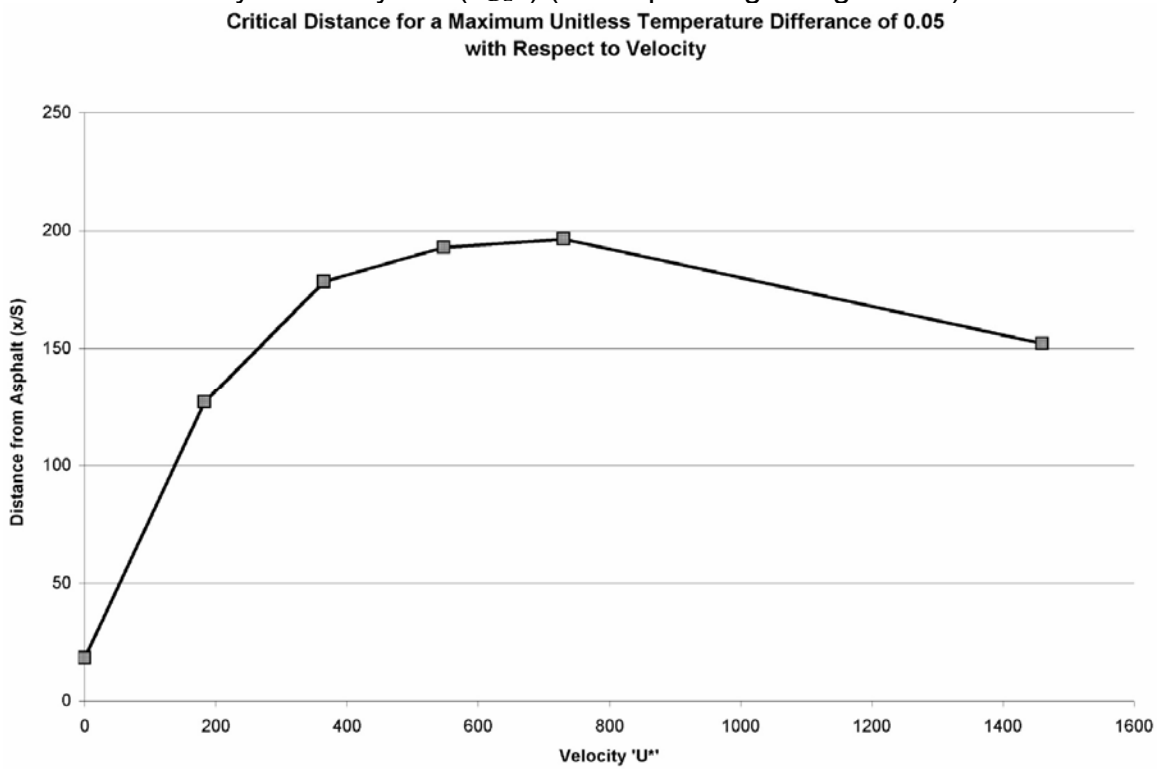Figure 5.7 Critical normalized distance from pavement (x*) vs. normalized groundwater flow velocity (U*) (corresponding to Figure 5.2).
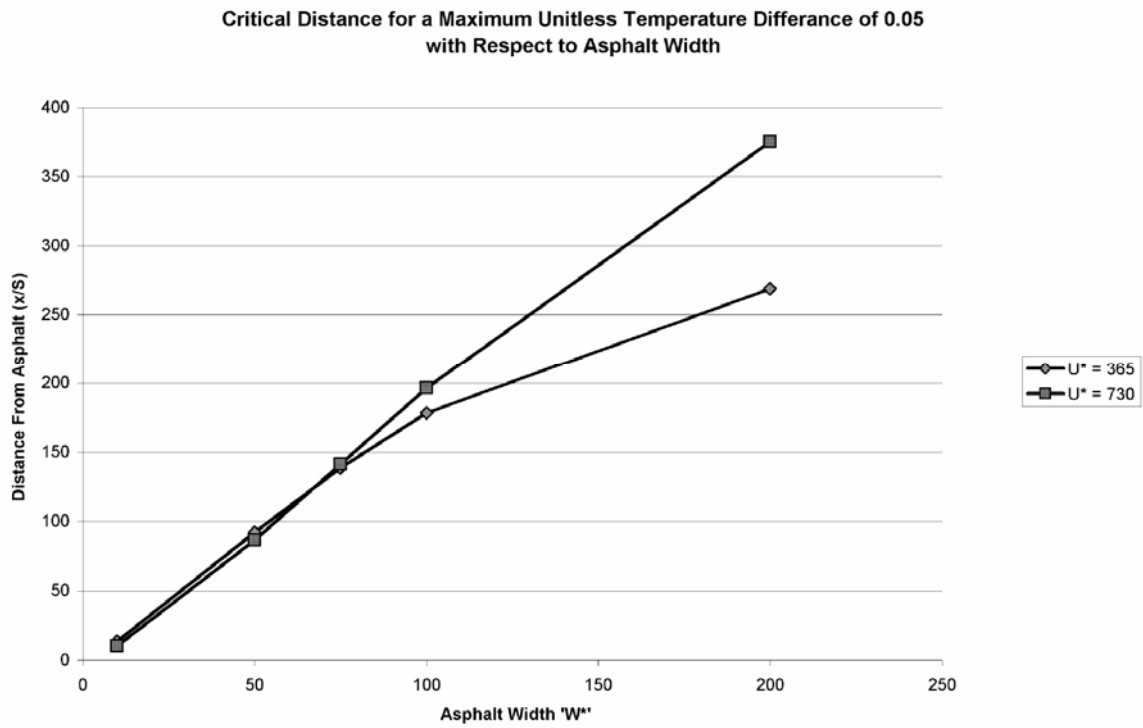
Figure 5.8 Critical normalized distance from pavement (x*) vs. normalized pavement width (W*) (corresponding to Figures 5.3 and 5.5).
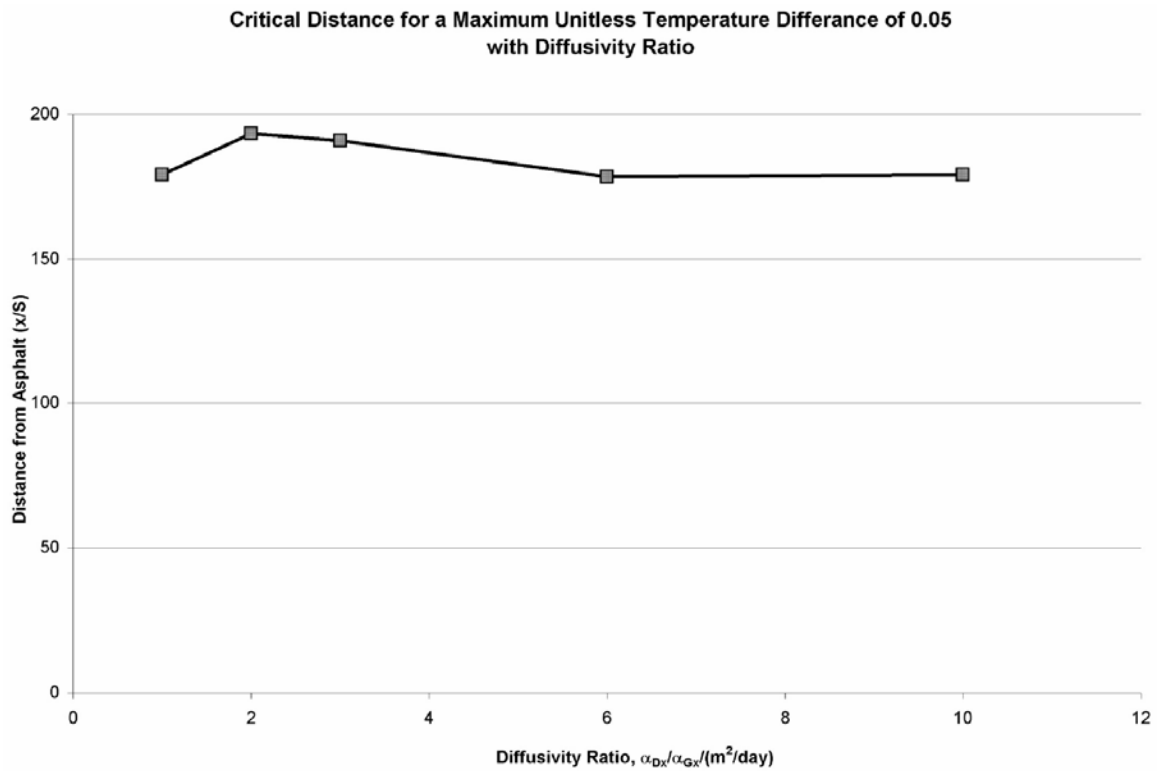
Figure 5.9 Critical distance from pavement (x^*) vs. diffusivity ratio in x-direction (α_{Dx}/α_{Gx}) (corresponding to Figure 5.4).

5.3 Application of numerical results

Figures 5.1 though 5.9 give some insight into the complex interactions and effects of climatic, soil and hydrologic parameters on the shape of an excess shallow groundwater temperature plume downstream from a "hot" parking lot surface simulated as an asphalt strip. Regulators need an answer to the question "How much horizontal distance is required from a paved surface to a coldwater stream such that the groundwater (temperatures) that discharges into the stream is not impacted by heat conduction and advection from the paved surface." It would be quite difficult (if not impossible) to develop a closed form expression for the critical distance that encompasses all of the controlling parameters. Instead we have simulated a wide range of practical cases. Because in all cases studied, and summarized in Figures 5.6 through 5.9, the critical distance is never greater than three times the width of the asphalt we propose that, for the chosen range of parameters, a reasonable approximation for the maximum critical distance is three times the width of the asphalt strip (paved surface).

6. Conclusions

The coldwater source of many coldwater streams is an aquifer. If the aquifer is shallow and can therefore be warmed from the ground surface, a coldwater stream may become warmer when the ground surface becomes warmer, e.g. by paving over previously vegetated land. We analyzed the heating of shallow groundwater when an asphalt strip is placed through a surface covered by grass only. The asphalt strip heats the soil and groundwater below and generates an excess temperature plume. Our analysis indicates that, for the range of parameters explored, a reasonable approximation of the maximum critical distance is three times the width of the asphalt strip. In other words, groundwater at a distance downstream larger than three times the width of the asphalt strip will experience a minimal impact from the presence of the warmer asphalt surface. This result provides a reasonable approximation of the buffer width that should be maintained between a coldwater stream and an asphalt surface, such as a parking lot.

Acknowledgements

References

Baker, J.M., and D.G. Baker (2002). "Long-term ground heat flux and heat storage at a mid-latitude site". *Climatic Change* 54:295-303.

Bear, J. (1972). *Dynamics of fluids in porous media.* American Elsevier Publishing Company, Inc., New York, 764pp.

Benekos, D.I. (2005). "On the determination of transverse dispersivity: Experiments and simulations in a helix and a cochlea". PhD dissertation, Department of Civil and Environmental Engineering, Stanford University, 122 pp.

Herb, W. R., Janke, B., Mohseni, O. and Stefan, H.G. (2006). "All-Weather Ground Surface Temperature Simulation". Project Report No. 478 St. Anthony Falls Laboratory, University of Minnesota, Minneapolis, MN, 57pp.

Hoffmann, Klaus A. and Chiang, Steve T. (2004) *Computational Fluid Dynamics Volume I Fourth Edition*. Engineering Education System, Wichita, Kansas

Qian, Q. and H.G. Stefan (2008).

Taniguchi, Makoto and Uemura, Takeshi. (2005). "Effects of urbanization and groundwater flow on the subsurface temperature in Osaka, Japan" *Physics of the Earth and Planetary Interiors* 152, 305–313

Taylor, C. A. and Stefan, H. G. (2008) "Shallow groundwater temperature response to urbanization and climate change: Analysis of heat transfer from the ground surface". Project Report No 504 Anthony Falls Laboratory, University of Minnesota, Minneapolis, MN, 73pp.

Zheng, C. and Bennett, G.D. (1995). *Applied contaminant transport modeling: theory and practice.* Van Nostrand Reinhold. New York.

Appendix A – Discretization of the governing equation

The dimensionless governing equation (5) can be solved numerically using an alternating direction implicit method with a central difference scheme spatially and a forward difference scheme temporally. This method solves for temperatures throughout the domain using two half time steps. The first half time step solves (updates) in the x-direction, while the second half time step solves in the y-direction. There are really two solution domains that are solved simultaneously. These domains are the region above the groundwater table (dry soil, subscript *"D"*) and the region below the groundwater table (groundwater, subscript *"G"*). The groundwater table itself can be thought of as a boundary. The two domains are both described by the same governing equation and solution. The only difference is that in the dry region there is no velocity term ($u*= 0$) and the diffusivities in the x-and y-directions are equal ($\alpha_{Dx} = \alpha_{Dy}$).

The discretization in the dry and groundwater domains is as follows.

First ½ time step:

$$\frac{T_{i.k}^{n+1/2} - T_{i.k}^{n}}{\Delta t / 2} + \frac{u*}{2\Delta x}\left(T_{i+1,k}^{n+1/2} - T_{i-1,k}^{n+1/2}\right) = \frac{\alpha_x*}{\Delta x^2}\left(T_{i+1,k}^{n+1/2} - 2T_{i.k}^{n+1/2} + T_{i-1,k}^{n+1/2}\right) + \frac{\alpha_z*}{\Delta z^2}\left(T_{i,k+1}^{n} - 2T_{i.k}^{n} + T_{i.k-1}^{n}\right)$$

$$\Rightarrow \left(\frac{-\alpha_x*}{\Delta x^2} - \frac{u*}{2\Delta x}\right)T_{i-1,k}^{n+1/2} + \left(\frac{2}{\Delta t} + \frac{\alpha_x*}{\Delta x^2}\right)T_{i.k}^{n+1/2} + \left(\frac{u*}{2\Delta x} - \frac{\alpha_x*}{\Delta x^2}\right)T_{i+1.k}^{n+1/2} \cdots$$

$$\cdots = \frac{2}{\Delta t}T_{i.k}^{n} + \frac{\alpha_z*}{\Delta z^2}\left(T_{i,k+1}^{n} - 2T_{i.k}^{n} + T_{i.k-1}^{n}\right)$$

$$\Rightarrow a_{xi}T_{i-1,k}^{n+1/2} + b_{xi}T_{i.k}^{n+1/2} + c_{xi}T_{i+1.k}^{n+1/2} = rhs_{xi}$$

Second ½ time step:

$$\frac{T_{i.k}^{n+1/2} - T_{i.k}^{n}}{\Delta t / 2} + \frac{u*}{2\Delta x}\left(T_{i+1,k}^{n+1/2} - T_{i-1,k}^{n+1/2}\right) = \frac{\alpha_x*}{\Delta x^2}\left(T_{i+1,k}^{n+1/2} - 2T_{i.k}^{n+1/2} + T_{i-1.k}^{n+1/2}\right) + \frac{\alpha_z*}{\Delta z^2}\left(T_{i,k+1}^{n+1} - 2T_{i.k}^{n+1} + T_{i.k-1}^{n+1}\right)$$

$$\Rightarrow \left(\frac{-\alpha_z*}{\Delta z^2}\right)T_{i,k-1}^{n+1} + \left(\frac{2}{\Delta t} + \frac{\alpha_z*}{\Delta z^2}\right)T_{i.k}^{n+1} + \left(-\frac{\alpha_z*}{\Delta z^2}\right)T_{i.k+1}^{n+1} \cdots$$

$$\cdots = \frac{2}{\Delta t}T_{i.k}^{n+1/2} + \frac{\alpha_x*}{\Delta x^2}\left(T_{i+1,k}^{n+1/2} - 2T_{i.k}^{n+1/2} + T_{i-1.k}^{n+1/2}\right) - \frac{u*}{2\Delta x}\left(T_{i+1,k}^{n+1/2} - T_{i-1,k}^{n+1/2}\right)$$

$$\Rightarrow a_k T_{i,k-1}^{n+1/2} + b_k T_{i.k}^{n+1/2} + c_k T_{i.k+1}^{n+1/2} = rhs_j$$

For any time step the boundary condition at the ground surface is a known temperature determined by equations (6 and 7). For the boundary condition at the bottom of the aquifer, Hoffmann and Chiang (2004) introduce a virtual

boundary that facilitates a second order accurate central difference discretization, which yields:

$$\frac{dT^*}{dz^*} = \frac{T^{*n+1}_{k_{MAX}+1} - T^{*n+1}_{k_{MAX}-1}}{2 \cdot \Delta z^*} = 0$$

$$\Rightarrow T^{*n+1}_{k_{MAX}+1} = T^{*n+1}_{k_{MAX}-1}$$

where k_{MAX}-1 denotes the point one step above the lower boundary
            k_{MAX}+1 denotes an imaginary point one step below the lower boundary

Equation (3.7) and the lower boundary condition result in the following tri-diagonal matrix:

$$\begin{bmatrix} b_2 & c_2 & & & & & \\ a_3 & b_3 & c_3 & & & & \\ & a_4 & b_4 & c_4 & & & \\ & & \ddots & \ddots & \ddots & & \\ & & & \ddots & \ddots & & \ddots \\ & & & & a_{k_{MAX}-1} & b_{k_{MAX}-1} & c_{k_{MAX}-1} \\ & & & & & a_{k_{MAX}} + c_{k_{MAX}} & b_{k_{MAX}} \end{bmatrix} \begin{bmatrix} T^{*n+1}_2 \\ T^{*n+1}_3 \\ T^{*n+1}_4 \\ \vdots \\ \vdots \\ T^{*n+1}_{k_{MAX}-1} \\ T^{*n+1}_{k_{MAX}} \end{bmatrix} = \begin{bmatrix} rhs_2 - a_2 \cdot T^{*n+1}_1 \\ rhs_3 \\ rhs_4 \\ \vdots \\ \vdots \\ rhs_{k_{MAX}-1} \\ rhs_{k_{MAX}} \end{bmatrix}$$

This tri-diagonal matrix can be numerically solved quite efficiently. Tri-diagonal matrix solver algorithms are readily available for most programming languages. The upper boundary condition is cyclical. This means that the initial condition throughout the rest of the domain is arbitrary because its effect on the solution will diminish over long enough time spans.